Elastodynamic behavior of the three dimensional layer-by-layer metamaterial structure

N. Aravantinos-Zafiris,[1] M. M. Sigalas,[1] and E. N. Economou[2]
[1]*Department of Materials Science, University of Patras, 26504 Patras, Greece*
[2]*Institute of Electronic Structure and Laser (IESL), Foundation for Research and Technology—Hellas (FORTH), P.O. Box 1385, Heraklion GR-71110, Greece and Department of Physics, University of Crete, Heraklion GR-71003, Greece*

(Received 13 June 2014; accepted 17 September 2014; published online 1 October 2014)

In this work, we numerically investigate for the first time the elastodynamic behavior of a three dimensional layer-by-layer rod structure, which is easy to fabricate and has already proved to be very efficient as a photonic crystal. The Finite Difference Time Domain method was used for the numerical calculations. For the rods, several materials were examined and the effects of all the geometric parameters of the structure were also numerically investigated. Additionally, two modifications of the structure were included in our calculations. The results obtained here (for certain geometric parameters), exhibiting a high ratio of longitudinal over transverse sound velocity and therefore a close approach to ideal pentamode behavior over a frequency range, clearly show that the layer-by-layer rod structure, besides being an efficient photonic crystal, is a very serious contender as an elastodynamic metamaterial. © *2014 AIP Publishing LLC*.
[http://dx.doi.org/10.1063/1.4896766]

I. INTRODUCTION

In the last thirty years, there is an intense research activity for the design of artificial composite materials endowed with novel properties not available in natural materials. Such properties aim at controlling the propagation of classical waves in unexpected and technologically exploitable ways. This rapidly developing field started with composite periodic structures, called photonic crystals, capable of creating frequency gaps (stop bands) in the propagation of electromagnetic (EM) waves and soon was extended to the propagation of elastic waves.[1,2] Initially, the elastic systems consisted of a periodic arrangement of scattering inclusions embedded in a homogeneous medium. This type of systems, called phononic crystals, have the ability, depending on the volume fraction and the contrast, to create band-gaps in their frequency response, which means that at a certain frequency range of the incident elastic (or acoustic) pulse the wave is completely reflected by the structure.[3–6] Several applications have been suggested such as in radio frequency communications,[7] microphononic crystal waveguides[8] and phononic crystal cavities and filters.[9–11] The next important development in this field was the concept and the fabrication of the so-called photonic metamaterials (see, e.g., Ref. 12), i.e., composite materials exhibiting features not found in their constituents or in other natural materials. Most of the photonic metamaterials are based on periodic artificial structures, whose unit cell exhibits strong resonance response. Such a response is responsible for the appearance of negative effective magnetic permeability, negative index of refraction, and a variety of other unexpected properties, which combined together gave rise to impressive behaviors such as invisibility cloacking and the development of transformation optics. Following these impressive developments for the propagation of EM waves in optical metamaterials, similar directions of research took place in the field of elastodynamics, that is the field of controlling the propagation and other features of elastic wave (see, e.g., Ref. 13) by the appearance of a variety of acoustic and elastodynamic metamaterials, i.e., composite structures that have novel elastic properties, which do not exist in their components or in other natural materials. In particular, Milton and Cherkaev[14,15] have shown that all mechanical materials can in principle be synthesized by combining pentamodes. Pentamodes are artificial special solids such that the ratio of the bulk modulus to the shear modulus is very large, ideally infinite. Pentamodes could be considered as the 3D elastodynamic counterpart of the 3D magnetodielectric metamaterials in optics. As such are capable in principles to implement 3D transformation elastodynamics and exhibit impressive behaviors such as acoustic cloaking.

Recently Kadic *et al.*[16] succeeded in fabricating, by using dip-in direct–laser-writing (DLW) optical lithography, 3D metamaterials approximating the pentamode ideal suggested by Milton and Cherkaev;[14] moreover, Martin *et al.* calculated[17] the phonon band structures for various parameters of this design and found ratios of velocities of longitudinal and transverse waves up to 16 for experimentally realizable structure parameters.

Although the work of Refs. 16 and 17 is impressive, their fabrication technique is rather complicated and not easily available. Thus, there is still the need to explore other designs approximating the pentamode ideal which are easier to construct and which may be proved capable to implement the elastodynamics transformation. Having this in mind, we numerically studied in this work a periodic structure based on the so-called layer-by-layer periodic structure which has a symmetry similar to that fabricated by Kadic *et al.*; this layer-by-layer periodic structure has been proved very

effective as a photonic crystal in 3D and easy to fabricate because of its layer-by-layer character.[18–20]

The structure, studied here for the first time as a candidate for desirable elastodynamics behavior, is shown in Figure 1. It consists of layers of one dimensional rods with a stacking sequence that repeats itself every four layers and the repeat distance is denoted by c. The distance between the centers of the rods within the layer is d and the width of each rod is w. Between adjacent layers, the orientation axis is rotated by 90° and between every other layer, the rods are shifted collectively by 0.5d. For the calculation of the band structure, the FDTD method was used. In the calculations only one unit cell was used with Periodic Boundary Conditions (PBC) along each direction of the unit cell as a result of the Bloch theorem. The size of the computational cell (which is identical to the unit cell) was d along the x and y directions and c along the z direction (see Fig. 1). The excitation, taken as a Gaussian pulse in time, was located at one low symmetry point of the unit cell. The components of the displacement vector as a function of time were collected in the detection point (in another low symmetry point of the unit cell). However, the results are not dependent on the location of the excitation or the detection point. Each component was Fourier transformed. The resulted spectrum consisted of well-defined resonant peaks that correspond to band structure points for the particular **k** vector. The dimensionless **k** vector components along the three examined directions in k-space are defined as $k_y = \frac{2\pi}{d}$, $k_z = \frac{2\pi}{c}$ and $k_{yz} = \frac{2\pi}{\sqrt{d^2+c^2}}$, respectively. Changing the **k** vector value used in the PBC, the band structure could be obtained. In our calculations, the highest value of the **k** vector was $0.5(2\pi/d)$ starting from 0 and the step size was 0.1. Due to the cubic grid used in the FDTD calculations, a 3D orthogonal lattice was used consisting of 60 by 60 by 80 grid points along x, y, and z axes, respectively.

The main goal of this work was to investigate the usage of this design as a 3D transformation elastodynamic structure. It is well known that the layer-by-layer structure has been already used as a 3D photonic crystal[18] and recently a numerical study showed that it could also worked as a phononic crystal.[21] Here, we focus on how well this structure can approach the pentamode ideal and examine how the different modes of the field are affected by changing several geometrical parameters of the structure. The phase velocities of the longitudinal and transverse waves propagating in the structure could be calculated from the slopes of the branches emerging from the Γ ($\mathbf{k} = 0$) point of the band structure. This is an accurate calculation assuming very small values of **k** vector (less than 10% of its maximum value) or, equivalently, very low values of the frequency. So the calculation of the phase velocities from the band structures could give information about the parameters of the structure that affects each velocity. Additionally, we examine how the response of the structure is affected by modifying it. Silicon, epoxy, and tungsten were the different materials considered for this structure. Table I contains the sound velocities and densities of the materials used in the calculations. Silicon is assumed to be an isotropic material for the calculations of this work.

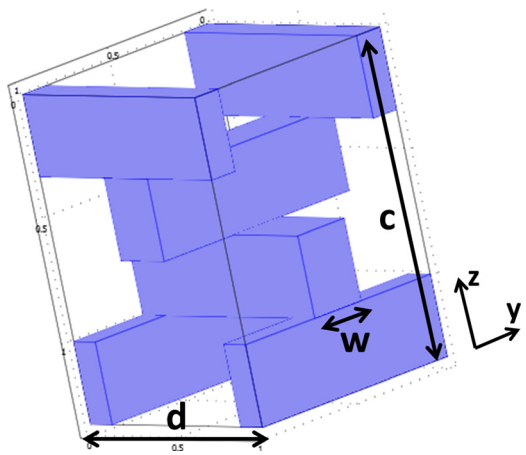

FIG. 1. The unit cell of the studied structure with its geometric properties.

For each material, numerical calculation was performed for different directions in k space. The stacking direction is chosen as the z-axis and the in plane directions are the x and y axes as shown in Fig. 1. It is important to mention here that x and y directions are by symmetry equivalent; for that reason only results for the k_y direction are shown. Notice that an incident longitudinal wave will develop in general transverse components as well, as it propagates through the structure; so it is more accurate to speak in general for "longitudinal-like" and "transverse-like" components of the field.

We conclude this introduction by pointing out once more that in order to create a structure suitable for three-dimension transformation elastodynamics and capable in principle of exhibiting impressive novel behaviors such as acoustic cloaking, we need solid composite materials for which the ratio of the "longitudinal-like" component over the "transverse-like" component to be as high as possible, ideally infinite. The calculations were performed assuming that the structure is embedded in air although the results should be almost the same if the solid material is in a vacuum considering the very low density of air.

II. RESULTS AND DISCUSION

A. Silicon

The first material combination considered in our calculations was silicon/air. It should be pointed that photonic crystals with similar dimensions as the ones studied here have been already fabricated.[20] The calculations were done for $d = 1\ \mu m$, c/d = 80/60 and for silicon rods of several values of w/d. It should be mentioned here that the results can be

TABLE I. The longitudinal (C_l), shear (C_t) sound velocities, and densities for the materials used in the calculations.

Material	C_l (km/s)	C_t (km/s)	Density (g/cm^3)
Silicon	8.43	5.84	2.34
Epoxy	2.54	1.16	1.18
Tungsten	5.20	2.90	19.4
Air	0.331	—	0.00129

scaled for other values of c, d, and w, assuming that the sound velocities and density are independent of frequency.

Firstly, we examined how the velocity of each component of the wave is affected by changing the ratio w/d. Table II contains the results of our calculations. We considered values for w/d equal 3/60, 7/60, 17/60, 21/60 and calculated the velocity of each component of the propagating wave. The ratio of the longitudinal wave velocity over the transverse velocity is also calculated in the last column of the table. In the same table, we show values of the angle between the propagation and the displacement vectors for the modes of interest in order to characterize quantitatively the terms longitudinal or transverse. The modes in this and the other tables and in various figures are characterized (for the sake of brevity) by the predominant component of the displacement field. We can clearly see that for w/d = 3/60 and the in plane direction the ratio C_l/C_t is almost 10. For the same direction and the same component, the ratio decreases as w/d increases.

We can also see that for w/d = 7/60 the ratio C_l/C_t has a value of 8.8 which is close to the corresponding ratio for the smaller w/d case. The interesting point for the ratio w/d = 7/60 is that, as shown in the band structure (Figure 2), a partial phononic band gap appears in both the stacking and the in-plane directions between 2 GHz and 3.3 GHz. Within this frequency range only a single longitudinal phonon mode appears for both directions. The disappearance of the transverse mode makes our structure an ideal pentamode in this frequency range. This opens up new avenues for transformation elastodynamics. For the ratio w/d = 7/60, the diagonal direction between y and z axes was also numerically examined. The relative direction is indicated as k_{yz} and the results are also collected in Table II. The partial phononic band gap also appears between 2 GHz and 3.3 GHz; moreover, for this direction only a single phonon mode is present. It is also obvious that even for this direction the ratio C_l/C_t remains high; thus we can conclude that in this frequency range, the proposed structure approaches an ideal pentamode behavior. Further calculations of the ratio C_l/C_t for the case of w/d = 7/60 at kd/2π = 0.5, i.e., the boundary of the Brillouin zone, lead to almost the same results further indicating the accuracy of the presented results. Our calculations continued by checking how the ratio C_l/C_t is affected by changing the stacking dimension of our structure. So, keeping w/d = 7/60, we proceeded to calculate for various values of c/d in order to examine the response of the structure to this parameter, starting from the initial ratio c/d = 80/60. The

TABLE II. Results of the silicon layer-by-layer structure (d = 1 μm, c/d = 80/60) for different w/d ratios. The modes were denoted by their predominant field component.

w/d	Direction	Field component	Slope	C_l/C_t	θ
3/60	k_y	x	0.52	9.90	
3/60	k_y	y	5.15		
3/60	k_y	z	0.75	6.87	
3/60	k_z	x	0.53	3.6	
3/60	k_z	y	0.53	3.6	
3/60	k_z	z	1.90		
7/60	k_y	x	0.66	8.8	86°
7/60	k_y	y	5.78		37°
7/60	k_y	z	1.18	4.9	86°
7/60	k_{yz}	x	1.14	5.1	83°
7/60	k_{yz}	y	5.87		64°
7/60	k_{yz}	z	2.23	2.6	42°
7/60	k_z	x	0.92	2.2	84°
7/60	k_z	y	0.88	2.3	84°
7/60	k_z	z	2.00		22°
17/60	k_y	x	1.27	4.7	
17/60	k_y	y	6.00		
17/60	k_y	z	1.84	3.3	
17/60	k_z	x	1.45	1.6	
17/60	k_z	y	1.32	1.7	
17/60	k_z	z	2.28		
21/60	k_y	x	2.19	2.8	
21/60	k_y	y	6.18		
21/60	k_y	z	2.70	2.3	
21/60	k_z	x	2.06	1.3	
21/60	k_z	y	2.00	1.4	
21/60	k_z	z	2.76		

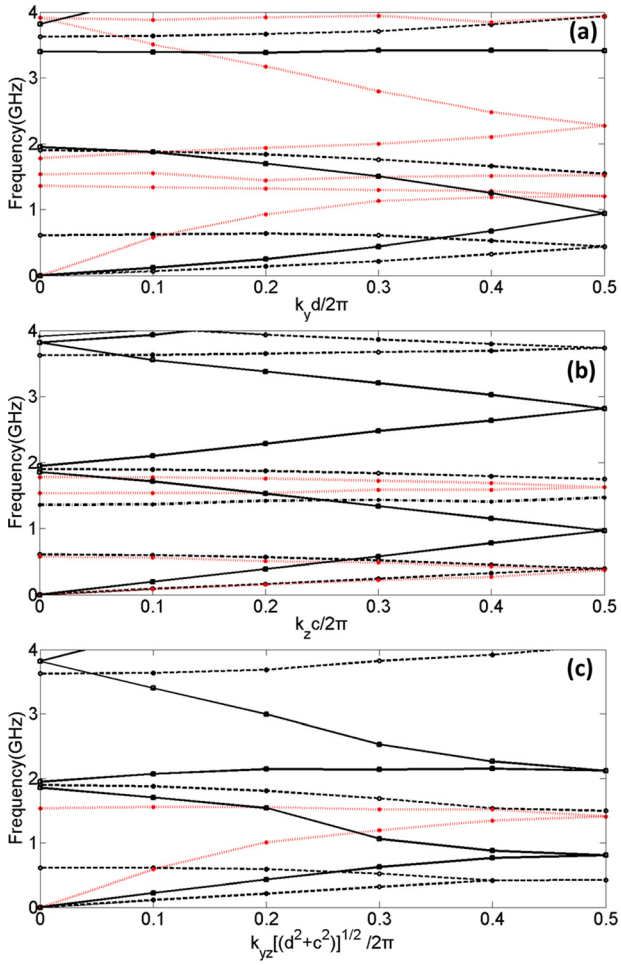

FIG. 2. The band structure of the silicon layer-by-layer phononic crystal (d = 1μm, c/d = 80/60, and w/d = 7/60) for propagation along each of three directions. The horizontal axis is the normalized k-vectors along each direction. (a) in-plane y-direction (which is the same as the x-direction due to symmetry), (b) stacking z-direction, (c) diagonal direction between y and z axes. Solid line is for the field component predominantly along the z-axis (stacking direction), dashed line is for the field component predominantly along the x-axis and red dotted (red) line is for the field component predominantly along the y-axis.

results are collected in Table III were we can see that decreasing c/d negatively affects (that is reduces) the ratio C_l/C_t. We calculated that for c/d = 80/60 along the in plane direction the longitudinal over the transverse component is propagating 8.8 times faster, whereas for c/d = 40/60 the same ratio is 6.7. Raising c/d to 120/60 the ratio C_l/C_t is also raised to 10.4. Note again that the results for the k_x direction are, by symmetry, equivalent with the ones along the ky direction.

In order to have a countable proof of the accuracy of our calculations and to check quantitatively the longitudinal-like and transverse-like character of the various eigenmodes, we proceeded to further calculate the inner product between the displacement vector **u** and the **k** vector for various eigenmodes in order to obtain the angle between them. This angle will indicate the longitudinal or the transverse or the mixed character of each mode. So for the case of w/d = 7/60 and for the eigenmodes along the y-direction and for $k_y d/2\pi = 0.05$ the angle between **u** and **k** was found to be 89° for both the transverse modes (one with **u** along the x-direction (at 0.035 GHz) and the other along the z-direction (at 0.057 GHz), i.e., very close to their ideal values. The third eigenmode (at 0.307 GHz) was longitudinal as expected forming an almost perfect angle of 6°. On the other hand, for the same direction but for $k_y d/2\pi = 0.1$ the angles between the **u** and **k** vectors for the three eigenmodes were found to be 86° for two of these modes with **u**, pointing almost completely along the x and z directions (at 0.066 GHz and 0.118 GHz, respectively) but 37° for the third mode (at 0.578 GHz) with **u** pointing mostly (not exclusively) along the y-direction. This indicates that two of the modes retain their almost ideally transverse character in spite of the rather large value of k_y, while the ideally longitudinal character of third mode has been lost. From the band structure (Fig. 2(a)), one can see that at $k_y d/2\pi = 0.1$ and 0.578 GHz the longitudinal-like mode crosses a transverse-like mode and a hybridized character takes place; this explains why the angle between **u** and **k** is far from the ideal (0°) for pure longitudinal character. In the case of $k_y d/2\pi = 0.05$ (Fig. 2(a)), there is no crossing between bands and for that reason both type of modes are close to their ideal values.

TABLE III. Results of the silicon layer-by-layer structure (d = 1 μm, w/d = 7/60) for different c/d ratios. The modes were denoted by the predominant field component.

c/d	Direction	Field component	Slope	C_l/C_t
120/60	k_y	x	0.53	10.4
120/60	k_y	y	5.52	
120/60	k_y	z	1.14	4.8
120/60	k_z	x	0.61	3.1
120/60	k_z	y	0.57	3.3
120/60	k_z	z	1.88	
80/60	k_y	x	0.66	8.8
80/60	k_y	y	5.78	
80/60	k_y	z	1.18	4.9
80/60	k_z	x	0.92	2.1
80/60	k_z	y	0.88	2.2
80/60	k_z	z	1.97	
60/60	k_y	x	0.88	6.8
60/60	k_y	y	5.96	
60/60	k_y	z	1.10	5.4
60/60	k_z	x	1.14	1.7
60/60	k_z	y	1.00	1.9
60/60	k_z	z	1.93	
40/60	k_y	x	0.92	6.7
40/60	k_y	y	6.13	
40/60	k_y	z	0.92	6.7
40/60	k_z	x	1.40	1.1
40/60	k_z	y	1.31	1.2
40/60	k_z	z	1.60	

For propagation along the z-direction and for a rather larger value of k_z, $k_z c/2\pi = 0.1$, the angle was found to be 84° for both x and y components (at 0.092 GHz and 0.088 GHz, respectively) and 22° for z component (at 0.2 GHz). This shows that the ideal transverse character of the two eigenmodes is almost preserved in spite of the rather large value of k_z. On the other hand, the longitudinal character of the third mode is not so well preserved; this is due to the fact that its eigenfrequency being close to other modes induces the mode to acquire a mixed character.

To further demonstrate that other close-by (in frequency) modes are responsible for the mixed character of eigenmodes for directions of high symmetry we examined also the case of propagation along the z-axis but for very large value of k_z, $k_z c/2\pi = 0.5$, i.e., at the edge of the Brillouin zone. The angle was found to be 87° for both the low frequency modes (at 0.372 GHz and 0.399 GHz) with the displacement vectors pointing almost parallel to the y and x directions respectively, and 2.5° for the third high frequency (at 0.968 GHz) mode. This almost ideal transverse or longitudinal character of the modes in spite of the extremely high value of k_z is due to the fact that these modes do not cross other bands (Fig. 2(b)). For that reason, they keep their almost ideal character (either transverse or longitudinal) even though they are at the edge of the Brillouin zone. An additional demonstration that the mixed character of a high-symmetry mode is mainly due to the vicinity of other modes is provided by the following example: For propagation along the y-direction and for $k_y c/2\pi = 0.5$ the angle was found 52° for the low frequency (at 0.44 GHz) mode, 12° for the high frequency (at 1.204 GHz) mode, and 67° for the intermediate frequency (at 0.942 GHz) mode.

Finally, for the k_{yz} direction, the transverse and the longitudinal character of the modes is not so well preserved as in the high-symmetry directions even for small values of k_{yz}; this, of course, is to be expected. As k_{yz} moves towards the edge of the Brillouin zone, the mixed character of the modes becomes more pronounced, because, as a general rule, the probability of encountering other modes of similar frequency is increasing. To be more specific, we considered propagation along the diagonal direction yz and for $k_{yz}[d^2 + c^2]^{1/2}/2\pi = 0.1$ (Fig. 2(c)): The angle was found to be 83° for the lowest frequency (at 0.114 GHz) mode with **u** pointing mostly along the x-direction (indicating an almost ideal transverse character in spite of the rather large value of k_{yz}), 42° for the next mode (at 0.223 GHz), and 64° for the highest frequency (at 0.587 GHz) mode indicating a considerably mixed character due to the vicinity of other modes. For even

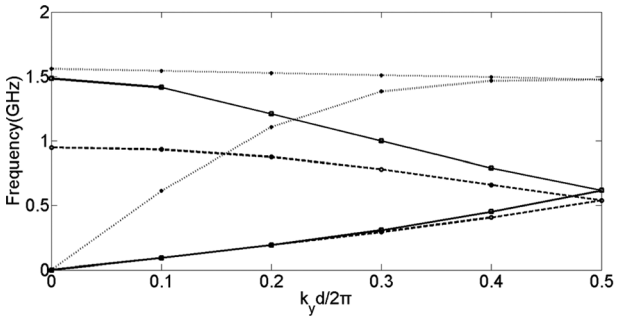

FIG. 3. The band structure of the silicon layer-by-layer phononic crystal (d = 1 μm, c/d = 40/60, and w/d = 7/60) along the in-plane y-direction. The horizontal axis is the normalized k-vectors. Solid line is for the mode with the predominant field component along the z-axis (stacking direction), dashed line is for the one with predominant field component along the x-axis and dotted line is the one with predominant field component along the y-axis.

larger value of k_{yz}, $k_{yz}[d^2+c^2]^{1/2}/2\pi = 0.5$, the angle was found 37° for both the lowest and the highest frequency (at 0.42 GHz and 1.41 GHz) modes and 19° for the intermediate frequency (at 0.805 GHz) mode.

Additionally, it is important to mention here that changing the dimension in the stacking direction has a noticeable effect on the mode denoted by the relative field component. Figures 3 and 4 show the band structure of the layer-by-layer phononic crystal for the two different directions (in plane and stacking direction, respectively) and for two different values of the c/d ratio (c/d = 40/60 and c/d = 80/60 at Figures 3 and 4, respectively). As one can clearly see from both figures, the z-component mode is clearly affected from this change. When the normalized k vector (x-axis) has a value 0.5 one of the modes is taking an obviously higher value compared to the rest modes for both in plane (Figure 3) and stacking direction (Figure 4).

Finally, as a final part of the study for silicon we examined two cases of a modified layer-by-layer structure in an attempt to obtain an improved elastodynamic behavior. Figure 5 shows the two different proposed modifications in the structure. The main change in the structure is that an amount of material is removed from each rod. In the first case, called here Modified Structure 1 (MS1), the material is removed from the place of the rod where it is overlapped with the rod of the above layer (Figure 5(b)), whereas in the second case, called here Modified Structure 2 (MS2), the material is removed from the place of the rod where there is no overlap (Figure 5(c)). In both cases, we keep w/d = 7/60 and c/d = 80/60. We numerically examined how each modification in the structure affects the propagation of the wave along the stacking and the in-plane direction, respectively.

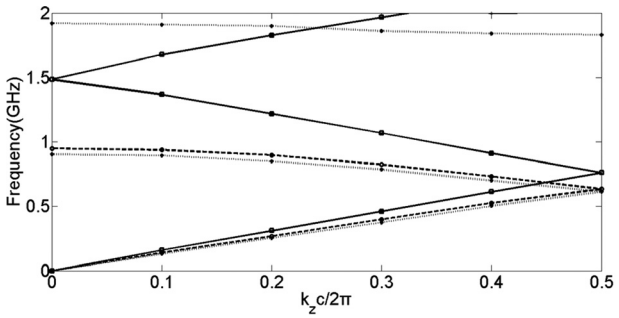

FIG. 4. The band structure of the silicon layer-by-layer phononic crystal (d = 1 μm, c/d = 40/60, and w/d = 7/60) along the stacking direction. The horizontal axis is the normalized k-vectors. Solid line is for the mode with predominant field component along the z-axis (stacking direction), dashed line is for the mode with predominant field component along the x-axis and dotted line is for the mode with predominant field component along the y-axis.

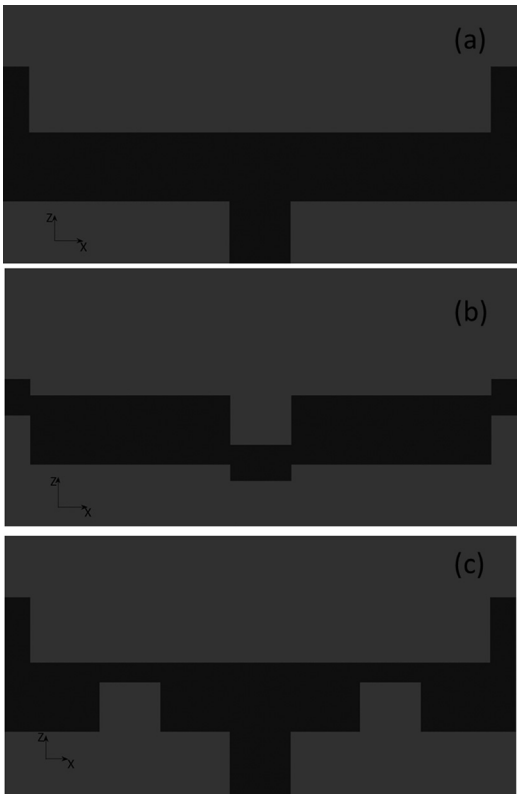

FIG. 5. Two proposed modified layer-by-layer structures. (a) A cross section of the x-z plane of the unmodified structure studied. (b) x-z plane of the Modified Structure 1 at the same y coordinate as in (a). Material is removed from each rod of all the layers from the parts of each rod that there is overlap with the rods from the above layer. (c) x-z plane of the Modified Structure 2 at the same y coordinate as in (a). Material is removed from each rod of all the layers from the parts of the rod that there is no overlap with the rods from the above layer. The same amount of material is removed from each rod in both cases.

Table IV contains the results of this part of our work together with the case where no material is removed from the rods (indicated as NM (No Modification)). It is clear again from the data that the in plane direction is the one that is mostly affected. As we can see, for the modified cases, the ratio C_l/C_t is about 4.4 vs 8.8 for the unmodified case. Figure 6 shows the band structure for the in plane direction for the NM and MS1 structures. It is obvious from those figures that the z component mode is negatively affected from the modification of the structure.

Summarizing the results for the silicon layer-by-layer case, it is obvious that this structure could give very interesting and promising results as an elastodynamic metamaterial structure, since both large ratio of C_l/C_t are produced and a frequency range is exhibited where the system behaves as an ideal pentamode. These aspects, together with the easiness of

TABLE IV. Results of the silicon layer-by-layer structure (d = 1 μm, w/d = 7/60, and c/d = 80/60) for different modifications of the layer-by-layer structure. The modes were denoted by their predominant field component.

Structure	Direction	Field component	Slope	C_l/C_t
NM	k_y	x	0.66	8.8
NM	k_y	y	5.78	
NM	k_y	z	1.18	4.9
NM	k_z	x	0.92	2.2
NM	k_z	y	0.88	2.3
NM	k_z	z	2.00	
MS1	k_y	x	0.57	4.8
MS1	k_y	y	2.71	
MS1	k_y	z	0.92	2.9
MS1	k_z	x	0.83	2.1
MS1	k_z	y	0.74	2.4
MS1	k_z	z	1.75	
MS2	k_y	x	0.70	4.9
MS2	k_y	y	3.46	
MS2	k_y	z	0.92	3.8
MS2	k_z	x	0.80	1.7
MS2	k_z	y	0.70	1.9
MS2	k_z	z	1.32	

fabricating the layer-by-layer design, make it a prime candidate for elastodynamic metamaterial.

Since the parameter that seems to affects mostly the behavior of the structure is the w/d ratio, (which means that the thickness of the rods plays a very important role), in the study of the rest two materials we only performed calculations for various values of the w/d ratio.

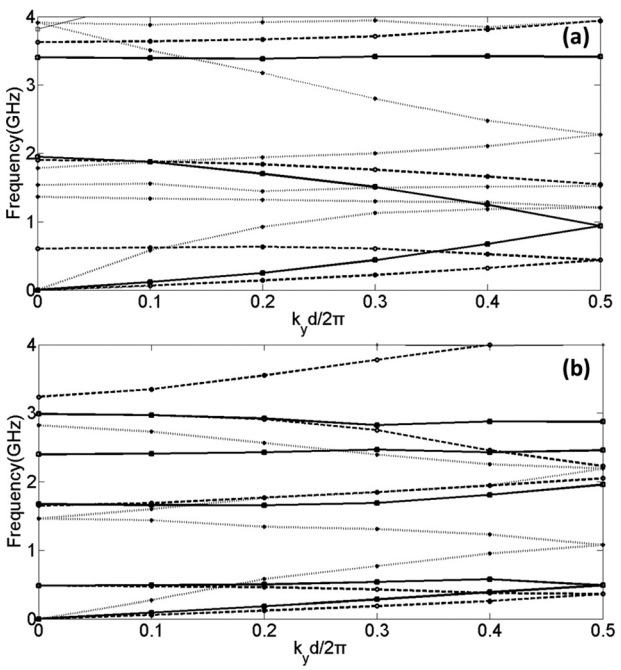

FIG. 6. The band structure of the Modified Structure 1 for silicon layer-by-layer phononic crystal (d = 1 μm, c/d = 80/60, and w/d = 7/60) along the three directions. The horizontal axis is the normalized k-vectors along each direction. (a) in-plane direction y and (b) stacking direction z. Solid line is for the mode with predominant field component along the z-axis (stacking direction), dashed line is for the mode with predominant field component along the x-axis and dotted line is for the mode with predominant field component along the y-axis.

B. Epoxy

The next material considered as the rod material is epoxy. As in the silicon case, the calculations took place by considering PBC for each direction in k space. Epoxy has a density that is almost half of silicon, so compared to the other materials examined in this work, it could be characterized as a "low density" material. Additionally, the sound velocities are several times lower than those of silicon. Table V shows the results for epoxy when d = 1μm, c/d = 80/60 and w/d varies as in the silicon case. From the results of Table V, it is clear that epoxy gives higher C_l/C_t ratio reaching the value 23.4 for w/d = 3/60. We can also see that increasing the ratio w/d reduces C_l/C_t. For the ratio w/d = 7/60 again a partial phononic band gap appears in both the stacking and the in-plane directions between 0.44 GHz and 0.75 GHz. Within this frequency range only a single longitudinal phonon mode appears for both directions. The disappearance of the transverse mode together with the ratio $C_l/C_t = 12.9$ for the same value of w/d makes our structure an almost ideal pentamode in this frequency range. Additionally, for the ratio w/d = 7/60, the diagonal direction between the y and z axes was also numerically examined. This direction, as in the silicon case, is indicated as k_{yz} and

TABLE V. Results of the epoxy layer-by-layer structure (d = 1 μm, c/d = 80/60) for different w/d ratios. The modes were denoted by their predominant field component.

w/d	Direction	Field component	Slope	C_l/C_t
3/60	k_y	x	0.05	23.4
3/60	k_y	y	1.17	
3/60	k_y	z	0.17	6.9
3/60	k_z	x	0.16	2.6
3/60	k_z	y	0.13	3.2
3/60	k_z	z	0.42	
7/60	k_y	x	0.17	12.9
7/60	k_y	y	2.20	
7/60	k_y	z	0.28	7.9
7/60	k_{yz}	x	0.26	5.2
7/60	k_{yz}	y	1.36	
7/60	k_{yz}	z	0.50	2.72
7/60	k_z	x	0.22	2.2
7/60	k_z	y	0.19	2.5
7/60	k_z	z	0.48	
17/60	k_y	x	0.29	4.8
17/60	k_y	y	1.39	
17/60	k_y	z	0.44	3.2
17/60	k_z	x	0.36	1.5
17/60	k_z	y	0.34	1.5
17/60	k_z	z	0.53	
21/60	k_y	x	0.48	3.0
21/60	k_y	y	1.45	
21/60	k_y	z	0.63	2.3
21/60	k_z	x	0.49	1.4
21/60	k_z	y	0.49	1.4
21/60	k_z	z	0.67	

the results are also collected in Table V. It is obvious that even for this direction the ratio C_l/C_t remains high. It is clear that in this frequency range the proposed structure approaches an ideal pentamode behavior.

C. Tungsten

The next material that was numerically examined is tungsten. Tungsten has a density that has a value almost ten times the density of silicon. So compared to the rest of the materials considered in this study it could be considered as a "high density" material. The results for tungsten are collected in Table VI. The calculations, as in the silicon case, are for $d = 1\ \mu m$, $c/d = 80/60$ and tungsten rods created in air for several values of w/d as shown in Table VI. A very interesting point for the ratio $w/d = 7/60$ is that a partial phononic band gap appears again in both the stacking and the in-plane directions between 1.2 GHz and 2.2 GHz. Within this frequency range only a single longitudinal phonon mode appears for both directions. The disappearance of the transverse mode together with the ratio $C_l/C_t = 7.5$ for the same value of w/d makes our structure an ideal pentamode in this frequency range. As in the previous cases of materials for the ratio $w/d = 7/60$ the diagonal direction between y and z axes was also numerically examined. This direction is indicated as k_{yz} and the results are collected in Table VI. It is obvious that for this direction also the ratio C_l/C_t remains high thus concluding that in this frequency range, the proposed structure approaches an ideal pentamode behavior.

TABLE VI. Results of the tungsten layer-by-layer structure ($d = 1\ \mu m$, $c/d = 80/60$) for different w/d ratios. The modes were denoted by their predominant field component.

w/d	Direction	Field component	Slope	C_l/C_t
3/60	k_y	x	0.27	16
3/60	k_y	y	4.32	
3/60	k_y	z	0.59	7.3
3/60	k_z	x	0.40	2.9
3/60	k_z	y	0.40	2.9
3/60	k_z	z	1.19	
7/60	k_y	x	0.43	7.5
7/60	k_y	y	3.24	
7/60	k_y	z	0.86	3.8
7/60	k_{yz}	x	0.86	3.8
7/60	k_{yz}	y	3.26	
7/60	k_{yz}	z	1.40	2.3
7/60	k_z	x	0.60	2.2
7/60	k_z	y	0.60	2.2
7/60	k_z	z	1.30	
17/60	k_y	x	0.86	4.0
17/60	k_y	y	3.46	
17/60	k_y	z	1.20	2.9
17/60	k_z	x	0.90	1.6
17/60	k_z	y	0.87	1.6
17/60	k_z	z	1.40	
21/60	k_y	x	1.30	2.7
21/60	k_y	y	3.57	
21/60	k_y	z	1.52	2.3
21/60	k_z	x	1.35	1.3
21/60	k_z	y	1.30	1.3
21/60	k_z	z	1.73	

III. SUMMARY

In conclusion, in this work, we examined for the first time the phononic metamaterial performance of the so-called layer-by-layer rod structure, which is well-known from the development of photonic crystals. In particular, we focused on the ability of this structure to act as an elastodynamic metamaterial, i.e., to be capable of performing transformation acoustic tasks such as acoustic cloaking. To perform such tasks one criterion is the ratio C_l/C_t of the longitudinal over the transverse sound velocity; this is essentially the figure of merit for any elastic metamaterial design. The other important criterion is the appearance of a frequency range in which the structure behaves as an ideal pentamode. Obviously, the easiness of fabrication of the structure is also an essential consideration. The present work shows that the layer-by-layer rod structure meets all these criteria to a satisfactory degree with a figure of merit C_l/C_t that can reach as high as 23. Thus, our results strongly suggest that this structure is a prime candidate for an elastodynamic metamaterial.

More specifically, in the present work, we examined three different component materials for the rods and all the geometrical parameters that could affect the behavior of the structure. We found that among the various parameters which affect the elastodynamic performance of the structure the most importance is the width of the rods. As the rods get thinner the structure becomes more functional as a metamaterial structure. Additionally the in-plane direction seems to be the direction for which the C_l/C_t ratio reaches the highest values. Two modifications of the structure based on removing material from each rod were also studied. These modifications seem to affect the component of the field which is on z direction without improving the performance.

Finally, it is important to mention here that the structure studied in this work can be easily fabricated with functionality both as photonic and as an elastodynamic metamaterial, a combination which may open uncharted directions.

ACKNOWLEDGMENTS

This work was supported by the ''Karatheodoris'' Research Program of the University of Patras.

This research has been co-financed by the European Union (European Regional Development Fund—ERDF) and Greek national funds through the Operational Program "Regional Operational Programme" of the National Strategic Reference Framework (NSRF)—Research Funding Program: Support for research, technology and innovation actions in Region of Western Greece.

E.N.E. acknowledges the financial support by the EU projects ENSEMBLE (Grant No 213669) and the Greek project ERC-02 ExEL (Grant No. 6260).

[1]M. M. Sigalas and E. N. Economou, J. Sound Vib. **158**, 377 (1992).
[2]M. S. Kushwaha, P. Halevi, L. Dobrzynski, and B. Djafari, Phys. Rev. Lett. **71**, 2022 (1993).

[3]M. Sigalas, M. S. Kushwaha, E. N. Economou, M. Kafesaki, I. E. Psarobas, and W. Steurer, Z. Kristallogr. **220**, 765–809 (2005).
[4]A. Srikantha Phani, J. Woodhouse, and N. A. Fleck, J. Acoust. Soc. Am. **119**(4), 1995–2005 (2006).
[5]E. M. Dede and G. M. Hulbert, Finite Elements Anal. Des. **44**, 819–830 (2008).
[6]O. R. Bilal and M. I. Hussein, Phys. Rev. E **84**, 065701 (2011).
[7]I. El-Kady, R. H. Olson III, and J. G. Fleming, Appl. Phys. Lett. **92**, 233504 (2008).
[8]R. H. Olsson III, I. F. El-Kady, M. F. Su, M. R. Tuck, and J. G. Fleming, Sens. Actuators A **145–146**, 87–93 (2008).
[9]J. C. Hsu and T. T. Wu, IEEE Trans. Ultrason. Ferroelectr. Freq. Control **53**, 1169–1176 (2006).
[10]A. Khelif, A. Choujaa, B. Djafari-Rouhani, M. Wilm, S. Ballandras, and V. Laude, Phys. Rev. B **68**, 214301 (2003).
[11]A. Khelif, P. A. Deymier, B. Djafari-Rouhani, J. O. Vasseur, and L. Dobrzynski, J. Appl. Phys. **94**, 1308–1311 (2003).
[12]C. M. Soukoulis and M. Wegener, Nature Photon. **5**, 523–530 (2011).
[13]*Acoustic Metamaterials and Phononic Crystals*, edited by P. A. Deymier (Springer, 2013) (see in particular the chapter by Jun Mei *et al*. on Dynamic Mass Density and Acoustic Metamaterials).
[14]G. W. Milton and A. Cherkaev, J. Eng. Mater. Technol. **117**, 483 (1995).
[15]G. Milton, *The Theory of Composites* (Cambridge University Press, Cambridge, UK, 2002), pp. 1-242.
[16]M. Kadic, T. Buckmann, N. Stenger, M. Thiel, and M. Wegener, Appl. Phys. Lett. **100**, 191901 (2012).
[17]A. Martin, M. Kadic, R. Schittny, T. Buckmann, and M. Wegener, Phys. Rev. B **86**, 155116 (2012).
[18]K. M. Ho, C. T. Chan, C. M. Soukoulis, R. Biswas, and M. Sigalas, Solid State Commun. **89**, 413–416 (1994).
[19]E. Özbay, G. Tuttle, J. S. McCalmont, M. Sigalas, R. Biswas, C. M. Soukoulis, and K. M. Ho, Appl. Phys. Lett. **67**, 1969–1972 (1995).
[20]S. Y. Lin, J. G. Fleming, D. L. Hetherington, B. K. Smith, R. Biswas, K. M. Ho, M. M. Sigalas, W. Zubrzycki, S. R. Kurtz, and J. Bur, Nature **394**, 251–253 (1998).
[21]N. Aravantinos-Zafiris and M. M. Sigalas, J. Vib. Acoust. **135**, 041003 (2013).